

Fig 2.2. Gating scheme for the PSSB PFC topology

III. OPERATIONAL PRINCIPLE

To analyze the circuit operation, the input line cycle is separated into positive and negative half-cycles

A. Positive Half-Cycle Operation

Referring to Fig 2.1, during the positive half-cycle, when the ac input voltage is positive, Q1 turns on and current flows through L1 and Q1 and continues through Q2 and then L2, returning to the line while storing energy in L1 and L2. When Q1 turns off, the energy stored in L1 and L2 is released as current flows through D1, through the load, and returns through the body diode of Q2/partially through Db back to the input

B. Negative Half-Cycle Operation

Referring to Fig.2.1, during the negative half-cycle, when the ac input voltage is negative, Q2 turns on and current flows through L2 and Q2 and continues through Q1 and then L1, returning to the line while storing energy in L2 and L1. When Q2 turns off, the energy stored in L2 and L1 is released as current flows through D2, through the load, and returns split between the body diode of Q1 and Da back to the input

C Detailed Positive Half Cycle Operation and Analysis for D>0.5

Interval 1: At t_0 , Q1 and Q2 are on, as shown in figure 3.1. During this interval, the current in series inductances L1 and L2 increases linearly and stores the energy in these inductors. The energy stored in Co provides energy to the load. The return current is split among Db, Dq2, and Q2.

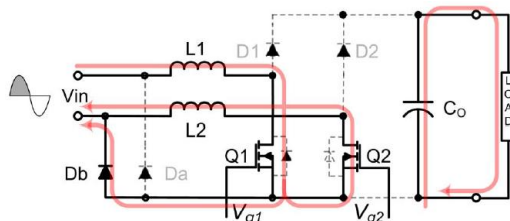


Fig.3.1. Intervals 1 and 3: Q1 and Q2 on

Interval 2: At t_1 , Q1 is on, and Q2 is off, as shown in Figure 3.2. During this interval, the current in series inductances L1 and L2 continues to increase linearly and store the energy in these inductors. The energy stored in Co provides the load energy. The return current is split only between Db and Dq2.

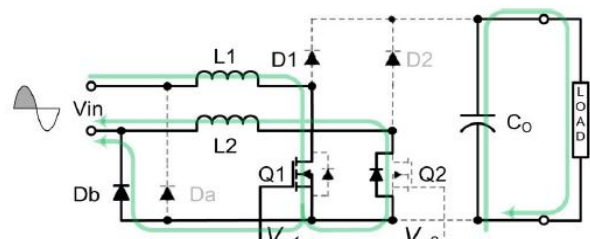


Fig.3.2 Interval 2: Q1 on body diode of Q2 conducting

Interval 3:

At t_2 , Q1 and Q2 are on again, and interval 1 is repeated, as shown in Figure 3.1. During this interval, the current in series inductances L1 and L2 increases linearly and stores the energy in these inductors. The return current is again split among Db, Dq2, and Q2.

Interval 4:

At t_3 , Q1 is off, and Q2 is on, as shown in Figure 3.3. During this interval, the energy stored in L1 and L2 is released to the output through L1, D1, partially Q2, Dq2, L2, and Db.

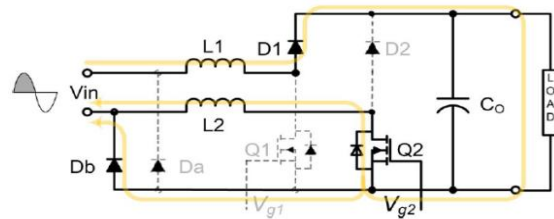


Fig.3.3. Interval 4: Q1 off and Q2 on

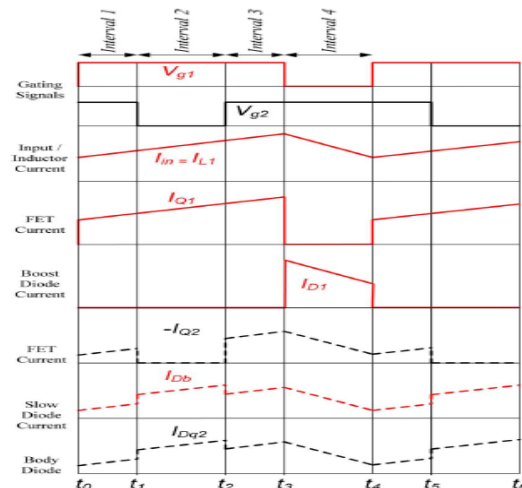


Fig.3.4. PSSB boost converter steady-state waveforms for D > 0.5

IV. SIMULATION ANALYSIS AND RESULT

The proposed converter is simulated and output waveforms are obtained. The converter input voltage is 200 V and output obtained is 400V.

The simulation analysis of the proposed converter is carried out on the basis of the following assumptions:

- 1) Input voltage (V_{in}) = 200V
- 2) Output voltage (V_o) = 400V
- 3) Switching frequency (f_s) = 50KHz
- 4) Duty ratio(D) = 53%

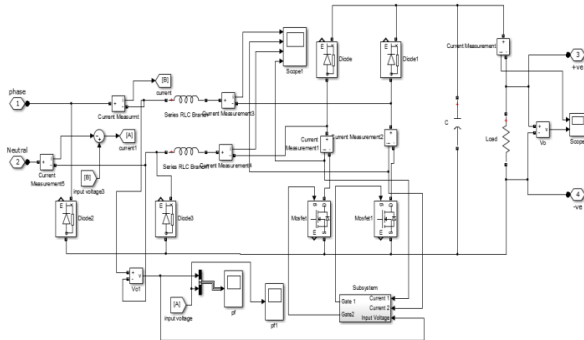


Fig.4.1. closed loop simulation diagram for PSSB converter

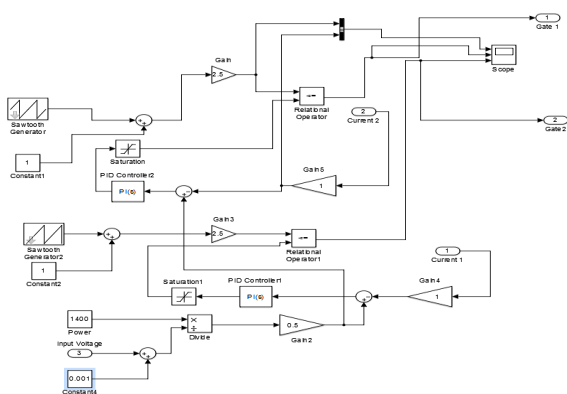


Fig.4.2. Sub system simulation diagram PSSB converter

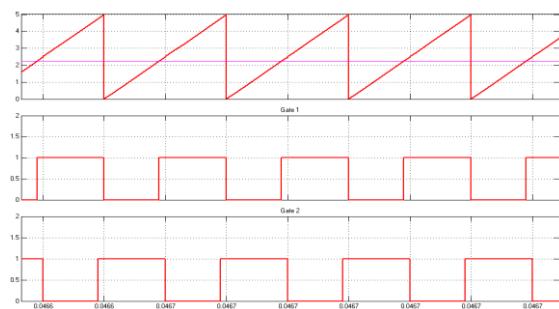


Fig.4.3. Generation of gate pulse in closed loop simulation

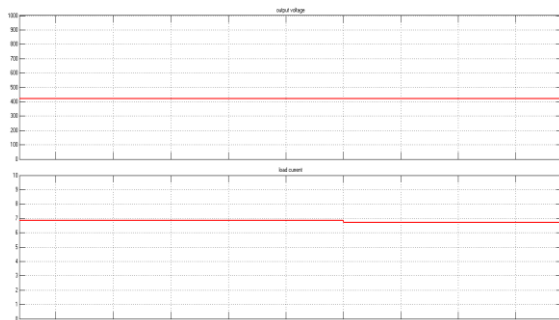


Fig.4.4. output voltage and load current

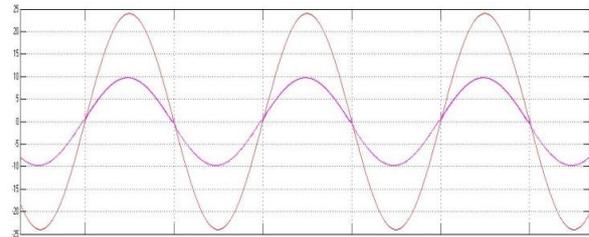


Fig.4.7. input current and input voltage in same phase

V.CONCLUSION

A high performance phase shifted semi bridgeless boost ac–dc boost PFC converter topology has been proposed to simplify the current sensing technique for the semi bridgeless PFC converter. The converter features high efficiency at light load and low line conditions, which is critical to minimize the charger size, cost, charging time, and amount and cost of electricity drawn from the utility. It provides higher efficiency at high power levels and solves the problem of heat management in the input rectifier diode bridge. Conduction losses are minimized due to the presence of only two semiconductor switches in any given conduction path. This converter is less bulky in comparison to the conventional topologies. The closed loop simulation and hardware prototype of the converter is done.

REFERENCES

- [1] J. Zhang, B. Su, and Z. Lu, “Single inductor three-level bridgeless boost power factor correction rectifier with nature voltage clamp,” *IET Power Electron.*, vol. 5, no. 3, pp. 358–365, Mar. 2012
- [2] M. Ramezani and S. M. Madani, “New zero-voltage-switching bridgeless P, using an improved auxiliary circuit,” *IET Power Electron.*, vol. 4, no. 6, pp. 732–741, Jul. 2011.
- [2] Interleaving Continuous Conduction Mode PFC Controller, Texas Instrum., Dallas, TX, Apr. 2011.
- [3] Y. J. Lee, A. Khaligh, and A. Emadi, “Advanced integrated bidirectional AC–DC and DC–DC converter for plug-in hybrid electric vehicles,” *IEEE Trans. Veh. Technol.*, vol. 58, no. 8, pp. 3970–3980, Oct. 2009.
- [4] Y. Jang and M. M. Jovanovic, “A bridgeless PFC boost rectifier with optimized magnetic utilization,” *IEEE Trans. Power Electron.*, vol. 24, no. 1, pp. 85–93, Jan. 2009.
- [5] T. Qi, L. Xing, and J. Sun, “Dual-boost single-phase PFC input current control based on output current sensing,” *IEEE Trans. Power Electron.*, vol. 24, no. 11, pp. 2523–2530, Nov. 2009.
- [6] K. Morrow, D. Karner, and J. Francfort, “Plug-in hybrid electric vehicle charging infrastructure review,” U.S. Dept. Energy—Veh. Technol. Program, Washington, DC, 2008.
- [7] P. Kong, S. Wang, and F. C. Lee, “Common mode EMI noise suppression for bridgeless PFC converters,” *IEEE Trans. Power Electron.*, vol. 23, no. 1, pp. 291–297, Jan. 2008
- [8] L. Huber, J. Yungtaek, and M. M. Jovanovic, “Performance evaluation of bridgeless PFC boost rectifiers,” *IEEE Trans. Power Electron.*, vol. 23, no. 3, pp. 1381–1390, May 2008.